ELSEVIER

Journal of Fluids and Structures 20 (2005) 621–641

JOURNAL OF FLUIDS AND STRUCTURES

www.elsevier.com/locate/jfs

Interaction of a rotational motion and an axial flow in small geometries for a Taylor–Couette problem

L.A. Bordag[a,*], O.G. Chkhetiani[b], M. Fröhner[c], V. Myrnyy[c]

[a]*Högskolan i Halmstad, Box 823, 301 18 Halmstad, Sweden*
[b]*Space Research Institute, Russian Academy of Sciences, Profsoyuznaya 84/32, 117997 Moscow, Russian Federation*
[c]*Fakultät Mathematik, Naturwissenschaften und Informatik, Brandenburgische Technische Universität Cottbus, Universitätsplatz 3/4, 03044 Cottbus, Germany*

Received 1 December 2003; accepted 27 January 2005
Available online 7 April 2005

Abstract

We analyze the stability of a Taylor–Couette flow under the imposition of a weak axial flow in the case of a very short cylinder with a narrow annulus gap. We consider an incompressible viscous fluid contained in the narrow gap between two concentric short cylinders, in which the inner cylinder rotates with constant angular velocity. The caps of the cylinders have narrow tubes conically tapering to very narrow slits, allowing an axial flow along the surface of the inner cylinder. The approximated solution for the Taylor–Couette flow for short cylinders was found and used for the stability analysis instead of the precise but bulky solution. The sensitivity of the Taylor–Couette flow to small perturbations and to weak axial flow was studied. We demonstrate that perturbations coming from the axial flow cause the propagation of dispersive waves in the Taylor–Couette flow. While in long cylinders the presence of an axial flow leads to the breaking of axial symmetry, in small cylinders it leads to the breaking of mirror symmetry. The coexistence of a rotation and an axial flow requires that, in addition to the energy and the angular momentum of the flow, the helicity must also be studied. The approximated form for the helicity formula in the case of short cylinders was derived. We found that the axial flow stabilizes the Taylor–Couette flow. The supercritical flow includes a rich variety of vortical structures, including a symmetric pair of Taylor vortices, an anomalous single vortex and quasiperiodic oscillating vortices. Pattern formation was studied at large for rated ranges of azimuthal and axial Reynolds numbers. A region where three branches of different states occur was localized. Numerical simulations in 3-D and in the axisymmetrical case of the model flow are presented, which illustrate the instabilities analyzed.

PACS: 47.32.−y; 47.20.−k; 47.54.+r

1. Introduction

Since Taylor's famous experiments in long cylinders (Taylor, 1923), many experimental and theoretical investigations of the interesting phenomena of the occurrence and evolution of Taylor vortices have been undertaken. The bulk of these studies was devoted to cases of long cylinders (Ludwieg, 1964; Joseph, 1976). This was done under the assumption

*Corresponding author. Tel.: +46 35 16 76 82; fax: +46 35 12 03 48.
E-mail addresses: Ljudmila.Bordag@ide.hh.se, ljudmila@bordag.com (L.A. Bordag).

0889-9746/$ - see front matter © 2005 Elsevier Ltd. All rights reserved.
doi:10.1016/j.jfluidstructs.2005.01.002

that a sufficiently long cylinder and periodic boundary conditions will emulate the infinitely long cylindrical region well. In addition, such regions are convenient for theoretical investigations. The simple form of the base flow was a fundamental part of Joseph's (1976) global stability analysis. The base flow, in the case of infinitely long cylinders, does not depend on the axial coordinate, and depends only on the radius.

The experimental investigations of short cylinders started much later and brought surprising results [see, for example, Mullin and Benjamin (1980), Benjamin and Mullin (1981), Benjamin and Mullin (1982)] which indicated that the zone and the magnitude of the influence of the caps of cylinders is much bigger and effects the kind of motion in the whole region. It was assumed that near the cylinders' caps the flow in the boundary layer is directed from the outer to the inner cylinder resulting from the existence of an Ekman boundary layer. The experiments, however, gave a more complicated picture of these motions. There exists also an atypical flow in the boundary layer in opposite direction, i.e. from the inner to the outer cylinder connected with the existence of the 'anomalous mode'. The first mathematical model which took the influence of the cylinder caps into account was the work of Schaeffer (1980). This model is not very consistent and needs improvement. The role of the anomalous mode was later studied numerically and experimentally in the works of Cliffe and Mullin (1985), Cliffe et al. (1992) and Streett and Hussaini (1991). The transient features of the circular Couette flow were investigated in laboratory and numerical experiments (using the commercial program 'Nekton' (Fluent GmbH) by Neitzel et al. (1995). The results of the numerical experiments were close to the laboratory experiments. In the case of short cylinders results with an aspect ratio $\Gamma\sim1$ (relation of the annulus span to the annulus gap width, defined in Section 2), usually only one pair of Taylor vortices emerged. In general, this case garners little interest, due to low expectations for the emerging patterns. The experiments of Aitta et al. (1985), Benjamin and Mullin (1981) however, found a series of interesting flow patterns for short cylinders. A non-equilibrium tricritical point occurs when a forward bifurcation becomes a backward bifurcation. In the Taylor–Couette problem the tricritical point can be observed for $\Gamma_T = 1.255$ in the classic case of pure rotation of the inner cylinder without axial flow, as demonstrated in Aitta et al. (1985) and later in Mullin et al. (2002), Streett and Hussaini (1991). The system of two vortices is symmetrical if the rotation velocity does not exceed a critical velocity v_1. If the velocity of the flow is larger, $v > v_1$, then one vortex grows at the expense of the other. In the case of forward bifurcation, symmetry is broken continuously; and in the case of backward bifurcation, abruptly. In phase transition language, this is a bifurcation of second order or first order, correspondingly (Bhattacharjee, 1987). The continuous transition was observed for $\Gamma < \Gamma_T$ and the abrupt one for $\Gamma_T < \Gamma < \Gamma_C$, where $\Gamma_C = 1.292$.

An exhaustive study of the influence of finite length effects has been made for the classic arrangement of two concentric cylinders with a very small aspect ratio $\Gamma \in [0.5, 1.6]$ and a relatively large annulus with a radius ratio (relation between the radii of inner and outer cylinders, see Section 2) of $\eta = 0.667$ for moderate Reynolds numbers $\mathrm{Re} \in [100, 1500]$ in the work of Furukawa et al. (2002) in cases when the inner cylinder is rotating. The numerical investigations were verified by experiments. The three main flow patterns they found correspond to a normal two-cell mode, an anomalous one-cell mode and a twin-cell mode. A steady case as well as an unsteady mode of fully developed flow that differs from wavy Taylor–Couette flows were obtained.

There exists a series of experimental and theoretical works devoted to the linear stability of the Taylor–Couette flow, which imposed axial effects. The first such analysis was done for cases of axisymmetric disturbances in a narrow gap (Chandrasechar, 1960; Di Prima, 1960). The work of Marques and Lopez (1997) analyzes the linear stability of the flow in the annulus between two infinitely long cylinders, driven by a constant rotation and harmonic oscillation in the axial direction of the inner cylinder using Floquet theory. The axial effects in the Taylor–Couette problem were studied in the work Meseguer and Marques (2000) on two different flows. In the first, the axial effect is introduced by an inertial axial sliding mechanism between the cylinders, and in the other, via an imposed axial pressure gradient. In all cases, the annular gap is much larger than in our case and the radius ratio is $\eta = 0.5, \ldots, 0.8$. The stabilizing effect of a periodic axial flow was studied in the works of Chandrasekhar (1961), Hu and Kelly (1995), and Weisberg et al. (1997). Ludwieg (1964) studied experimentally cases of very long cylinders with an aspect ration of $\Gamma = 80$ and a radius ratio of $\eta = 0.8$, as well as an axial flow that fills full cross sections between the cylinders. In his work Ludwieg describes the breaking of axial symmetry which did not take place in our case.

In the work of Lueptow (2000) the stability problem of a Taylor–Couette flow with axial and radial flow was studied for a relatively large radius ratio $\eta = 0.83$ and pressure-driven axial flow in the whole annulus. It was found in all these studies that the axial flow stabilized the Taylor–Couette flow and enabled a multitude of supercritical states with a rich variety of patterns.

Nevertheless, the theory of the Taylor–Couette flow is far from complete, as, for instance, the stability problem in the system of Taylor vortices and classic Couette flow as subject to the influence of cylinder caps was not investigated. It is also a bit astonishing that the exact analytical solution for the azimuthal component of the Taylor–Couette flow profile with boundary conditions on cylinder caps was obtained just recently in the work of Wendl (1999). His results expose the strong influence of caps on flow profiles. For a wide range of radius ratios η, the difference between the two profiles

(with and without finite-length effects) is approximately a logarithmic function of the aspect ratio Γ. The solution is given in the form of a slowly convergent series containing trigonometric and Bessel functions. To give a qualitative analysis of instabilities, one takes an exact solution as a base flow to linearize the Navier–Stokes equations. This type of solution is not convenient for further analytic studies of instabilities.

In the present work, we use the theory of small perturbations to study the instability of the laminar Taylor–Couette flow in a short cylinder. The geometry of an annular gap and the boundary conditions are given in Section 2. Our idea was to find an analytical formula for the azimuthal component which is simpler than that in Wendl (1999) but one that can still give us an approximation of the Taylor–Couette flow with finite-length effects as good as those found in Wendl (1999). In Section 3 we describe this solution and discuss the region of applicability of the found approximation.

The solution obtained for a short cylinder is quite suitable as a base flow for a comprehensive study of instability effects. This study is represented in Section 4. The onset of instability is predicted using the method of local analysis. In this method, the equations governing the flow perturbation are linearized. Exactly because the appearance of instability depends not only on the base flow but also on the amplitude and type of flow perturbations, two different types of perturbations are studied in this section. We investigated the basic flow just before bifurcation appeared, and the main emphasis of our work was to investigate which physical phenomena lead to instabilities in the flow. The base flow in our case is strongly inhomogeneous in the axial direction, and Joseph's method cannot be applied to such a base flow.

The consideration of the sensitivity of the Taylor–Couette flow regarding small perturbations corresponding to an axial flow is most important for industrial applications. We take the case of a very narrow annulus $\eta\sim1$ that is typical for bearing or sealing systems and, contrary to general expectation, we find a rich family of flow states. We prove that the axial flow also stabilizes the Taylor–Couette flow in cases with a very short cylinder and narrow annular gap with axial flow in a thin layer directed along the surface of the inner rotating cylinder.

The elaborate series of numerical experiments was done with the help of FLUENT 5.5/6.0. Detailed descriptions of the grids used and other numerical facilities are given in Section 6.

The change from one laminar flow to another, or a transition from a laminar flow to turbulence, is a function of the base flow as well as the type of small perturbations. We found a rich family of typical patterns in large intervals of Reynolds numbers. The results of the numerical experiments are discussed in Section 7.

2. The main problem

The study of the Taylor–Couette problem for the parameters defined below was stimulated by an industrial project (Bordag, 2001). In many technical systems the problem of transmitting energy and momentum is solved using shafts and corresponding bush bearing systems with or without radial sealing. In a typical situation, one is concerned with a small Taylor–Couette annulus, narrow slits between cylinders and with axial and tangential oscillations or with a weak axial flow along the surface of the inner cylinder. In general, these systems are very complicated and it is necessary to study simpler problems in order to isolate a particular mechanism and to develop and test hypotheses governing their behavior. We chose here only one of the most typical cases for its technological importance and, from a fundamental point of view, for its rich dynamics and in order to try to describe all possible flow states in this case.

We consider the motion of the fluid in an annulus between two cylinders as represented in Fig. 1.

The annulus dimensions are: gap width d, annulus span l, radius of the inner cylinder r_{in}, an outer cylinder r_{out}. The corresponding dimensionless geometric parameters are the aspect ratio $\Gamma = l/d$ and the radius ratio $\eta = r_{\text{in}}/r_{\text{out}}$. We use these notations throughout the paper. For many sealing or bearing systems $\Gamma\sim1$ and $\eta\sim1$. In all of our calculations we fix $\Gamma = 1.02$, $\eta = 0.95356$.

We assume that the inner cylinder will turn at the constant rate ω. The outer cylinder is at rest, the axial flow has a constant velocity w_0 and we assume $r_{\text{in}}\omega \gg w_0$. The equations of fluid motion and boundary conditions will be rendered dimensionless using d, as a length scale. The radius of the inner cylinder shall be denoted by $R = r_{\text{in}}/d$ in dimensionless units; this shall be used in all sections of this paper.

The ingoing and outgoing gaps for the axial flow are very thin cylindrical slits, with the gap width denoted by $\tilde{d}$ and the annulus span of slits denoted by $\tilde{l}$. The slits are long and narrow in comparison to the main annulus i.e. $l\sim\tilde{l}$, $d \gg \tilde{d}$. The ends of the slits narrow conically to the lower order of scale, which means the narrowest part of the slit has the width $\tilde{\tilde{d}}$, which is very small, $d \gg \tilde{d} \gg \tilde{\tilde{d}}$. A more detailed picture of the slits is given in Fig. 7. The studied flow states are very sensitive to perturbations. Therefore, we try to construct a situation which is most adapted to technical facilities or physical experimental possibilities and imitate the sealing arrangements with conically tapering slits.

It is characteristic for technical applications that the sealing medium be oil with non-vanishing viscosity. In our work we shall consider an incompressible viscous fluid in the cylindrical annulus.

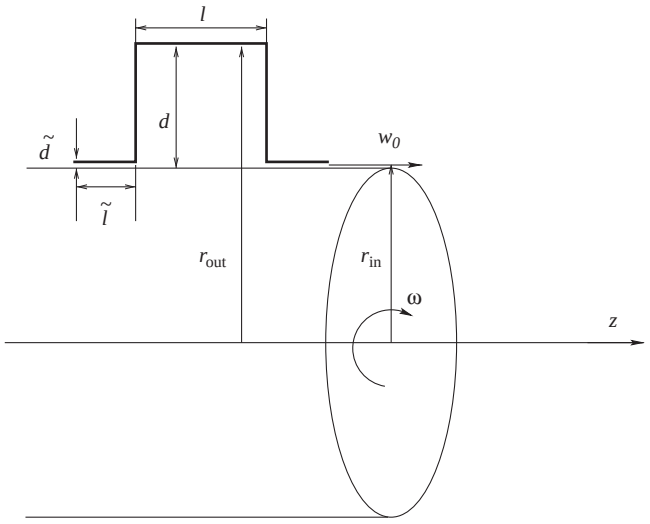

Fig. 1. The geometry of the annulus. The radii of the inner and outer cylinders are equal to r_{in}, r_{out} correspondingly; the annulus span is denoted by l, the annular gap width is $d = r_{out} - r_{in}$. The corresponding geometrical parameters of the slits are denoted by $\tilde{d}$ and $\tilde{l}$. Other notations are explained in the text.

3. An approximation of the exact solution in cases of a rotating inner cylinder

The classic case of the Taylor–Couette flow of incompressible viscous fluid in an annulus between two cylinders was investigated analytically in Wendl (1999). In comparison to the famous work of Taylor (1923), the author studied cylinders of a finite length, thus finding a much more complicated formula for the azimuthal component of the Taylor–Couette flow which describes the influence of cylinder caps on the flow. As understood from the experiments of Ji et al. (2001) and Kageyama et al. (2004) if the Reynolds number grows, the influence of the Ekman layer drops along the cylinder caps. As a result, the profile of the solutions becomes more and more different from the pure Taylor–Couette solution due to the emergence of secondary flows in the annulus.

Wendl (1999) did not mention any physical conditions for the applicability of his solutions. He implicitly assumed that the Taylor–Couette flow in a short cylinder is an unidirectional axial symmetric steady flow and got an exact solution for the azimuthal component of the flow. This solution will be an exact solution of the Navier–Stokes equations in the limit of small Reynolds numbers only.

With analytical and numerical methods we estimated the radial and axial components of the velocity in the Taylor–Couette flow, as shown later in our work. These components are small compared with the azimuthal component. This, the basic Taylor–Couette flow is thereby almost unidirectional for short cylinders with $\Gamma \sim 1$ and radius ratio $\eta \sim 1$.

We shall consider the flow in the annular gap with width d, span l, and radius of inner cylinder r_{in} as on the Fig. 1 without slits. We suggest now that the caps of the cylinders contact the inner cylinder and that there is no axial flow in the annulus. The equations of the fluid motion and the boundary conditions will be rendered dimensionless using $v = r_{in}\omega$ and $P = \rho(v/d)^2 = \rho v v/d$ as units for velocity and the pressure. Scalings of the velocities and of other quantities shall change from section to section.

Let us study the azimuthal component of the Taylor–Couette flow in a short cylinder. Due to the axial symmetry two of the components of the velocity vector $\mathbf{u}(r, \theta, z)$ vanish in this case and the velocity vector reads

$$\mathbf{u}(r, z) = (0, V_0(r, z), 0), \tag{1}$$

where $V_0(r, z)$ is the azimuthal component. That is, we look for the leading term in the expansion of the velocity vector in respect to the Reynolds number. The cylindrical Navier–Stokes equations can be reduced in this model to one equation,

$$\frac{\partial^2 V_0}{\partial r^2} + \frac{1}{R+r}\frac{\partial V_0}{\partial r} - \frac{V_0}{(R+r)^2} + \frac{1}{\Gamma^2}\frac{\partial^2 V_0}{\partial z^2} = 0. \tag{2}$$

The boundary conditions can be rendered dimensionless as

$$V_0(r,0)=0,\quad V(r,1)=0,\quad V_0(0,z)=1,\quad V_0(1,z)=0,\quad z\in[0,1],\quad r\in[0,1]. \tag{3}$$

We make an additional scaling in the z-direction by Γ in order to reach a more convenient condition in which both variables r and z lie in the interval $[0,1]$. The case considered was solved by Wendl (1999) using the Fourier transformation. The solution has the following form:

$$V_0(r,z)=\frac{1}{4\pi}\sum_{m=1}^{\infty}\frac{(\mathrm{I}_1(\beta_m(R+1))\mathrm{K}_1(\beta_m(R+r))-\mathrm{K}_1(\beta_m(R+1))\mathrm{I}_1(\beta_m(R+r)))\sin(\beta_m z)}{(2m-1)(\mathrm{I}_1(\beta_m(R+1))\mathrm{K}_1(\beta_m R)-\mathrm{K}_1(\beta_m(R+1))\mathrm{I}_1(\beta_m R))} \tag{4}$$

with $\beta_m=(2m-1)\pi/\Gamma$. Here I_1 and K_1 are modified Bessel functions. This solution differs drastically from the simple solution obtained by Taylor for the infinitely long cylinders. However, this solution remains an exact solution also for long cylinders as it was in case of short cylinders. The series in Eq. (4) converges very slowly and it is difficult to apply in comprehensive studies. We therefore looked for simpler analytic representations of this solution or for some substantial approximated solution.

We study the case of short cylinders, i.e. $\Gamma\sim1$, with a narrow gap, $\eta\sim1$, and $R\gg1$. Under these assumptions and taking into account $r\in[0,1]$, we can simplify the initial equation (2) by replacing $1/(R+r)$, $1/(R+r)^2$ with the constants $1/R$, $1/R^2$. For the simplified equation with constant coefficients, we obtain the solution in a closed analytical form,

$$V_0(r,z)=\frac{2}{\pi}\arctan\left(\left(\sinh^{-1}\left(\frac{\pi}{\Gamma}r\right)-\sinh^{-1}\left(\frac{\pi}{\Gamma}(2-r)\right)\right)\sin(\pi z)\right), \tag{5}$$

in which $r\in[0,1]$ and $z\in[0,1]$. This is a convenient form of the approximated solution for the fundamental mode of the Taylor–Couette flow profile which we will use in what follows.

Agreement between the approximated and the exact solutions is very strong, as can be seen in Fig. 2. We used also the program FLUENT 5.5/6.0 in the axisymmetric case to calculate the corresponding solution of the full system of Navier–Stokes equations. The azimuthal component of this solution is given on the same Fig. 2. The very good agreement between azimuthal components in all cases studied confirm the assumption that the flow in this system is quite unidirectional.

The approximated solution (5) is stable for small Reynolds numbers Re and can be used as a base state in a stability analysis.

We note an earlier attempt by Vladimirov et al. (2001) to find an approximated solution which takes the influence of the caps into account; the results, however, are farther from the exact solution than ours.

4. Stability problem for the Taylor–Couette flow under small perturbations

4.1. Local stability study for a short cylinder

We consider the axisymmetrical stability problem of the Taylor–Couette flow. We assume that the velocity vector $\tilde{\mathbf{u}}(r,z)$ which describes the fluid motion in the annular gap such as in Fig. 1 can be represented as a sum of two vectors $\mathbf{u}(r,z)=(u,v,w)$ and $\mathbf{v}(r,z)=(0,V_0,0)$:

$$\tilde{\mathbf{u}}(r,z)=\mathbf{v}(r,z)+\mathbf{u}(r,z)=(0,V_0,0)+(u,v,w), \tag{6}$$

where V_0 describes the fundamental mode of the Taylor–Couette flow and $\mathbf{u}(r,z)$ a perturbation of this mode. We assume also that the pressure $\tilde{P}$ can be represented as sum $\tilde{P}=P_0+p$.

Under the following assumptions

$$\max_{r,z}|\mathbf{v}(r,z)|\gg\max_{r,z}|\mathbf{u}(r,z)|,\quad \max_{r,z}\frac{|\nabla\mathbf{u}|}{|\mathbf{u}|}\gg\max_{r,z}\frac{|\nabla\mathbf{v}|}{|\mathbf{v}|}, \tag{7}$$

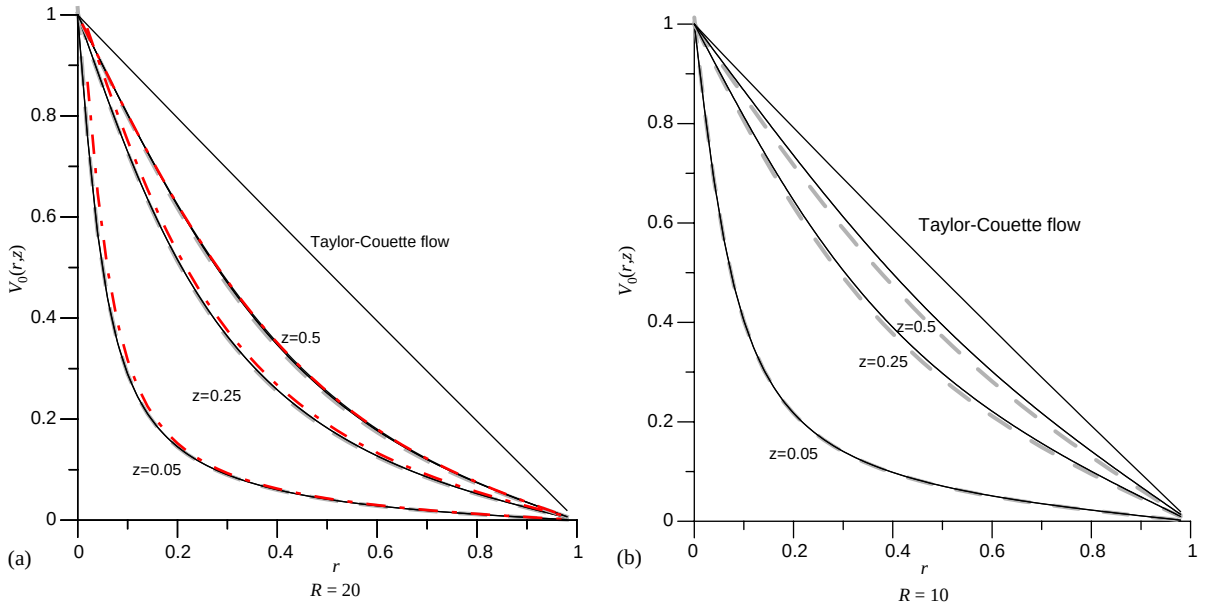

Fig. 2. The profiles $V_0(r,z)$ of the exact (dashed line), the approximate solutions (continuous line) and numerical solution (dash-dotted line) as functions of r on z-levels equal to $z = 0.05, 0.25, 0.5$ with $\Gamma = 1$. The numerical solution was found with program FLUENT 5.5/6.0 in axisymmetric case for $\mathrm{Re} = 100$.

in which ∇ denotes the spatial gradient of the corresponding velocity, the system of the Navier–Stokes equations can be linearized. The linearized Navier–Stokes equations (LNSE) in the axisymmetrical case take the form

$$\begin{aligned}
&\partial_t u - 2\,\mathrm{Re}\,\frac{vV_0}{R+r} = -\partial_r p + \Delta u - \frac{u}{(R+r)^2},\\
&\partial_t v + \mathrm{Re}\left(\partial_r V_0 u + \frac{V_0}{R+r}\,u + \partial_z V_0 w\right) = \Delta v - \frac{v}{(R+r)^2},\\
&\partial_t w = -\frac{1}{\Gamma^2}\,\partial_z p + v\Delta w,\\
&\partial_r u + \frac{u}{R+r} + \partial_z w = 0,
\end{aligned} \tag{8}$$

where Δ is the Laplace operator,

$$\Delta = \partial_{rr} + \frac{\partial_r}{R+r} + \frac{\partial_{zz}}{\Gamma^2}. \tag{9}$$

The Reynolds number is $\mathrm{Re} = \omega r_{\mathrm{in}} d/v$, and v denotes the viscosity of the fluid. The dimensionless variables r, z which describe the flow in the cylindrical annulus belong to the intervals

$$r \in [0,1], \quad z \in [0,1]. \tag{10}$$

Here we use the dimensionless variables as introduced in the Section 2 and in addition, we use the value d^2/v and $r_{\mathrm{in}}\omega$ to render time and velocities dimensionless as well. We leave the same notations as above for the velocities in the dimensionless case. Thus, now $|V_0| \sim 1$ and it follows from conditions (7) that $|v| \ll 1$.

We shall introduce a commonly used stream function Ψ for cases of axial symmetry [see Milne-Thomson (1996)]

$$u = \frac{\partial_z \Psi}{R+r}, \quad w = -\frac{\partial_r \Psi}{R+r}. \tag{11}$$

In terms of the stream function Ψ and the azimuthal velocity v the LNSE of Eqs. (8) turn into a system of two coupled equations

$$\begin{aligned}
&\partial_t\widetilde{\Delta}\Psi - \frac{\mathrm{Re}}{\Gamma^2}\left(\frac{2\partial_z V_0}{R+r}\,v + \frac{2V_0}{R+r}\,\partial_z v\right) = \Delta\widetilde{\Delta}\Psi - \frac{\widetilde{\Delta}\Psi}{(R+r)^2},\\
&\partial_t v + \mathrm{Re}\left(\left(\partial_r V_0 + \frac{V_0}{R+r}\right)\frac{\partial_z\Psi}{R+r} - \partial_z V_0\,\frac{\partial_r\Psi}{R+r}\right) = \Delta v - \frac{v}{(R+r)^2}.
\end{aligned} \tag{12}$$

We note that the value $\widetilde{\Delta}\Psi$ is an azimuthal vorticity Υ_θ defined by

$$\Upsilon_\theta = \widetilde{\Delta}\Psi = \frac{1}{\Gamma^2}\,\partial_z u - \partial_r w, \quad \text{where } \widetilde{\Delta} = \frac{\Delta}{R+r}. \tag{13}$$

The basic Taylor–Couette flow is an axial inhomogeneous flow in cases of short cylinders, due to the influence of the cylinder caps. This inhomogeneity leads to additional terms which distinguish between system (8) and the corresponding linearized Navier–Stokes equations for an infinitely long cylinder. We shall now prove that these additional terms cause the propagation of dispersive waves in the Taylor–Couette flow.

We bear in mind that, in the case of a short cylinder with very narrow gap,

$$\Gamma\sim 1, \quad \eta\sim 1, \quad R\gg 1. \tag{14}$$

Under these assumptions we can simplify the system of equations (12) by replacing the coefficients $1/(R+r)^n$ (note $r\in[0,1]$) with the constants $1/R^n$, $n=1,2$. The operators ∂_z and ∂_r can be replaced by the multiplicative operators $\partial_r\sim 1/d$, $\partial_z\sim 1/l$ or, in the dimensionless case, by

$$\frac{\partial}{\partial r}\sim 1, \quad \frac{\partial}{\partial z}\sim\frac{1}{\Gamma} \tag{15}$$

due to Eqs. (10) and (14). Furthermore, we assume

$$\frac{\partial V_0}{\partial r} \gg \frac{V_0}{R+r} \tag{16}$$

and neglect $V_0/(R+r)$ in system (12). We shall now collect the leading terms in Eqs. (12) only and obtain a simplified system of equations

$$\begin{aligned}
&\partial_t\Delta\Psi - 2\mathrm{Re}\,\partial_z V_0 v - 2\mathrm{Re}\,V_0\partial_z v = \Delta^2\Psi,\\
&\partial_t v + \delta\mathrm{Re}\,\partial_r V_0\partial_z\Psi - \delta\mathrm{Re}\,\partial_z V_0\partial_r\Psi = \Delta v,
\end{aligned} \tag{17}$$

in which no-slip boundary conditions $u|_S = v|_S = w|_S = 0$ on the inner surface S of the annulus are adopted. In system (17) we denote $\Delta = \partial_{rr}^2 + \Gamma^{-2}\partial_{zz}^2$, and the constant $\delta\equiv 1/R$ is small, $\delta\ll 1$.

The standard, straightforward way to investigate the stability problem consists is in finding exact solutions of the eigenvalue problem corresponding to the system of equations (17). Thus the perturbation $\mathbf{u}(r,z)$ can be represented as a series over the eigenfunctions. Alternatively, the system could be solved numerically wherein spatial discretization of the problem may be accomplished by a solenoidal Galerkin scheme. In our case these procedures may be accomplished numerically only, but this task is outside the scope of the present work. The quantitative investigation cannot, however, change the principal physical picture of transition.

Nonetheless, we can produce good qualitative characteristics of the flow in the annulus by applying local stability analysis. This method was first developed in the analysis of an inhomogeneous complex astrophysical flow (Goldreich and Schubert, 1967; Lebovitz and Lifschitz, 1993). The method of local qualitative analysis has been used to study hydrodynamical systems for the last 10 years [see the works Lifschitz (1991), Lifschitz and Hameiri (1993) whose subjects are close to our work]. Very similar methods were used in Meseguer (2002), Hristova et al. (2002) in a study of subcritical transitions of the Taylor–Couette flow in the case of counter-rotating cylinders. This method allows us to investigate the main physical processes of the concerned Taylor–Couette flow, the transition mechanism and transition states.

The main idea of the local stability analysis method (also called a method of infinitesimal perturbations) can be described as follows. We suppose the amplitude and gradients of the main state (the fundamental mode of the Taylor–Couette flow in our case) to be preserved under perturbations. This means we keep the values $V_0, \partial_z V_0$ and $\partial_r V_0$ unaltered; that is, we assume they are constant. For all components of the perturbation vector $\mathbf{u}(r,z) = (u,v,w)$ and their derivatives, Taylor series truncated after the first two terms shall be used. Regarding the physical point of view, we assume that the perturbation scale is much smaller than the typical scale of the axial inhomogeneity in the Taylor–Couette system. This is the locality condition. As other investigators have done, we present the

perturbation as a plane wave,

$$\Psi \sim \widehat{\Psi}\exp(\gamma t + \mathrm{i}(k_r r + k_z z)), \quad v \sim \widehat{v}\exp(\gamma t + \mathrm{i}(k_r r + k_z z)), \tag{18}$$

in which $\widehat{\Psi}$ and $\widehat{v}$ are the amplitudes of the waves. The vector of wavenumbers $k = (k_r, k_z)$ defines the spatial direction of the plane wave propagation. The locality condition requires that $k_r, k_z \gg 1$. In Eqs. (18), γ has the dimension of a frequency; in stability analysis it is referred to as the time increment (or simply increment). In the case of intrinsic instability of the investigated system, γ will be positive. This means that the amplitude of the plane wave will infinitely increase with time.

The substitution of the plane wave Eqs. (18) into the linearized system (17) results in a system of algebraic equations for the increment γ,

$$-k^2(\gamma + k^2)\widehat{\Psi} - 2\frac{\mathrm{Re}}{\Gamma^2}(\partial_z V_0 + \mathrm{i}V_0 k_z)\widehat{v} = 0, \quad (\gamma + k^2)\widehat{v} + \mathrm{i}\delta\mathrm{Re}\,(\partial_r V_0 k_z - \partial_z V_0 k_r)\widehat{\Psi} = 0,$$

where $k^2 = k_r^2 + \Gamma^{-2}k_z^2$. This system can be solved explicitly, and two solutions for the increment γ can be obtained:

$$\gamma_\pm = -k^2 \pm \frac{\mathrm{Re}\,(2\delta)^{1/2}|k_z\partial_r V_0 - k_r\partial_z V_0|^{1/2}}{\Gamma k}(k_z^2 V_0^2 + (\partial_z V_0)^2)^{1/4} \times\left(\cos\left(\frac{1}{2}\arctan\left(\frac{\partial_z V_0}{k_z V_0}\right)\right) - \mathrm{i}\,\sin\left(\frac{1}{2}\arctan\left(\frac{\partial_z V_0}{k_z V_0}\right)\right)\right). \tag{19}$$

As a consequence, two different regimes of motion can exist in this system.

The motion in the annulus is strongly inhomogeneous in the z-direction due to the influence of the cylinder caps. Let us now look for local increments on the middle surface $r = 0.5$ on three different lines $z = 0.25,\ 0.5,\ 0.75$. For $z = 0.5$, the increment has no imaginary part and on this line the system shows no oscillations. In this case the real part of the increment is represented in Fig. 5. On the lines $z = 0.25,\ 0.75$ the increment has an imaginary part and the system has oscillations with frequencies directly proportional to the gradient of the undisturbed state.

For $\partial_z V_0 = 0$ we find two real solutions for the increment and, consequently, two branches of non-oscillating solutions.

The two branches of the increment given by Eq. (19) may also have an oscillating character. For $\partial_z V_0 \neq 0$ we must address two oscillating solutions which correspond to waves of the inertial type. If in addition $k_z\partial_r V_0 - k_r\partial_z V_0 = 0$ holds, then these two oscillating branches have a point of intersection. The intersection point $\gamma_\pm = -k^2$ is associated with a time-decreasing solution. On the other hand, perturbations with $k_z\partial_r V_0 - k_r\partial_z V_0 \approx 0$ have the possibility to exchange energy.

4.2. Local stability of the Taylor–Couette flow under a small axial perturbation flow

To date, the study of the stability problem of the Taylor–Couette flow concerned arbitrary small perturbations. Let us consider the effects of an axial flow near the surface of the inner cylinder. This flow can be generated by the pair of Taylor vortices or an axial flow through the narrow slits in the caps of the cylinders near the surface of the inner cylinder as shown in Fig. 1.

In order to simplify the study we suggest that the axial velocity $w(r, z)$ has a nonzero value $w(R, z)$ on the surface of the inner cylinder. Additionally, we suggest that the boundary condition is homogeneous in the z-direction, i.e. $w(R, z) = \zeta = \mathrm{const}$ holds. We can neglect here the dependence on the z-coordinate. The constant constituent of the axial velocity distribution can be removed by a Galilean transformation $z' = z - \zeta(1 + R)t$; $z' \to z$. The boundary condition $w(R, z) = \zeta \neq 0$ provides, via the narrow gap approximation, the linear velocity profile in the r-direction

$$w \approx \zeta(1 - (r - R)) = \zeta(1 + R) - \zeta r. \tag{20}$$

Now we can rewrite the LNSE, Eqs. (8), in the form

$$\partial_t\widetilde{\Delta}\Psi - \zeta\mathrm{Re}\,r\partial_z\widetilde{\Delta}\Psi + \frac{\zeta\mathrm{Re}\,\partial_z\Psi}{(R + r)^2} - \frac{2\mathrm{Re}\,\partial_z V_0}{\Gamma^2(R + r)}v - \frac{2\mathrm{Re}\,V_0}{\Gamma^2(R + r)}\partial_z v = \Delta\widetilde{\Delta}\Psi - \frac{\widetilde{\Delta}\Psi}{(R + r)^2},$$

$$\partial_t v - \zeta\mathrm{Re}\,r\partial_z v + \mathrm{Re}\left(\partial_r V_0 + \frac{V_0}{R + r}\right)\frac{\partial_z\Psi}{R + r} - \mathrm{Re}\,\partial_z V_0\frac{\partial_r\Psi}{R + r} = \Delta v - \frac{v}{(R + r)^2}.$$

We shall now simplify this system of equations, keeping in mind that we are investigating the influence of small perturbations and from conditions (7) it follows immediately that $\zeta \ll V_0$ or $\zeta \ll 1$. We expand the coefficients in the system into a series with respect to the parameter $\delta = 1/R$ and preserve only the main terms. The approximated system

for the stream function Ψ and for the azimuthal velocity v has the structure

$$\partial_t \Delta\Psi - \zeta \mathrm{Re}\, r\partial_z \Delta\Psi + \zeta\delta \mathrm{Re}\, \partial_z \Psi - \frac{2\mathrm{Re}}{\Gamma^2}\,\partial_z V_0 v - \frac{2\mathrm{Re}}{\Gamma^2} V_0 \partial_z v = \Delta^2 \Psi,$$
$$\partial_t v - \zeta \mathrm{Re}\, r\partial_z v + \delta \mathrm{Re}\, \partial_r V_0 \partial_z \Psi - \delta \mathrm{Re}\, \partial_z V_0 \partial_r \Psi = \Delta v. \tag{21}$$

As noted in the previous Section 4.1 we shall study the stability problem under small local perturbations. Thus the perturbation scale is much smaller than a typical scale of inhomogeneity in the system. This locality condition implies the inequalities

$$k_r \gg 1, \quad k_z \gg 1.$$

Following the same path, we can postulate that the values $V_0, \partial_z V_0$ and $\partial_r V_0$ will change very slowly as compared to perturbations. In that way, they can be represented by a Taylor series which is truncated after the first two terms. As usual, we assume that the perturbation $\mathbf{u}(r,z) = (u,v,w)$ has the form of a wave with time dependent amplitudes and with time-dependent wavenumber in the r-direction,

$$\Psi = \widehat{\Psi}(t)\exp(\mathrm{i}(k_r(t)r + k_z z)),$$
$$v = \widehat{v}(t)\exp(\mathrm{i}(k_r(t)r + k_z z)), \tag{22}$$

in which Ψ is the stream function (11) and v is the azimuthal velocity. The substitution of formulas (22) into the system of equations (21) leads to the simplified system of equations

$$-\partial_t((k_r^2(t) + k_z^2/\Gamma^2)\widehat{\Psi}(t)) - \mathrm{i}(\partial_t k_r(t) - \zeta \mathrm{Re}\, k_z) r(k_r^2(t) + k_z^2/\Gamma^2)\widehat{\Psi}(t)$$
$$+ \mathrm{i}\zeta\delta \mathrm{Re}\, k_z \widehat{\Psi}(t) - \frac{2\mathrm{Re}}{\Gamma^2}(\partial_z V_0 + \mathrm{i} V_0 k_z)\widehat{v}(t) = (k_r^2(t) + k_z^2/\Gamma^2)^2 \widehat{\Psi}(t), \tag{23}$$

$$\partial_t \widehat{v}(t) + \mathrm{i}(\partial_t k_r(t) - \zeta \mathrm{Re}\, k_z) r\widehat{v}(t) + \mathrm{i}\delta \mathrm{Re}(\partial_r V_0 k_z - \partial_z V_0 k_r)\widehat{\Psi}(t) = -(k_r^2(t) + k_z^2/\Gamma^2)\widehat{v}(t).$$

The solution of this system can be found for all r if the condition

$$\partial_t k_r(t) - \zeta \mathrm{Re}\, k_z = 0, \tag{24}$$

is fulfilled, because only two terms in system (23) have coefficients which depend on the variable r. Eq. (24) can be solved easily and we find that

$$k_r(t) = k_r(0) + \zeta \mathrm{Re}\, t k_z. \tag{25}$$

The radial component k_r of a wavenumber vector $\mathbf{k}$ increases or decreases linearly, depending upon the sign of the axial component k_z of the wavenumber vector. In other words, we can explain the action of the axial shear as a change of the radial scale.

The time dependence of the wavenumber $k_r(t)$ leads to an algebraic non-exponential evolution which can be described by the system of equations

$$-\partial_t((k_r^2(t) + k_z^2/\Gamma^2)\widehat{\Psi}(t)) + \mathrm{i}\zeta\delta \mathrm{Re}\, k_z \widehat{\Psi}(t) - \frac{2\mathrm{Re}}{\Gamma^2}(\partial_z V_0 + \mathrm{i} V_0 k_z)\widehat{v}(t) = (k_r^2(t) + k_z^2/\Gamma^2)^2 \widehat{\Psi}(t),$$
$$\partial_t \widehat{v}(t) + \mathrm{i}\delta \mathrm{Re}\,(\partial_r V_0 k_z - \partial_z V_0 k_r)\widehat{\Psi}(t) = -(k_r^2(t) + k_z^2/\Gamma^2)\widehat{v}(t). \tag{26}$$

Perturbations such as studied here were considered in fluid dynamics since the work of Lord Kelvin, but only recently has it been realized that these perturbations can act as a trigger in subcritical turbulence transition. The untypical properties of our flow originate from the fact that the corresponding LNSE operator is not self-adjoint, as is usual for shear flows such as: plane Couette flow [see Lominadze et al. (1988), Buttler and Farrel (1992)], Poiseuille flow (Reddy and Hennigson, 1993), counter-rotating Taylor–Couette flow (Meseguer, 2002; Hristova et al., 2002), boundary layer (Gustavsson, 1979), Kepler rotation (Lominadze et al., 1988). Apart from the modes of the discrete spectrum, there exist many modes of the discontinuous spectrum. The algebraic time evolution of these modes can achieve large amplitudes which can reach a 100-fold of the initial values. Another remarkable property of these modes is their trait to redistribute the energy and momentum between different types of perturbations (Chagelishvili and Chkhetiani, 1995; Chagelishvili et al., 1996). In order to give a qualitative description of the impact from an axial flow on the stability of the Taylor–Couette flow we will find the increment for a fixed instant time. Analogous to Eqs. (18), we have the representation

$$\widehat{\Psi}(t) \sim \exp(\gamma t), \qquad \widehat{v}(t) \sim \exp(\gamma t) \tag{27}$$

for time-dependent amplitudes of wave (22). If we hold the time dependence of $k_r(t)$ virtually unaltered, we can consider the stability analysis as local in time. The substitution of formula (27) into the system of equations (26) leads to an algebraic equation for the increment. In this system we now have two solutions for the time increment γ

$$\gamma_{\pm} = -k^2 + \frac{\mathrm{i}\zeta\delta \mathrm{Re}\, k_z}{2k^2} \pm \frac{\mathrm{Re}\,\delta^{1/2}(64k^4\Lambda^2(\partial_z V_0)^2 + (\zeta^2\delta k_z^2 + 8k^2 k_z V_0\Lambda)^2)^{1/4}}{2\Gamma k^2}\exp(-\mathrm{i}\Phi), \tag{28}$$

$$\Lambda = k_z\partial_r V_0 - k_r\partial_z V_0, \quad \Phi = \frac{1}{2}\arctan\left(\frac{8k^2\partial_z V_0\Lambda}{\zeta^2\delta k_z^2 + 8k^2 k_z V_0\Lambda}\right).$$

For small ζRe, the dispersion curves have the same form as acknowledged in the previous section (without any axial flow). In the intersection area $k_z\partial_r V_0 - k_r\partial_z V_0 \approx 0$ we now have

$$\gamma_+ = -k^2 + \frac{\mathrm{i}\zeta\delta \mathrm{Re}\, k_z}{2k^2}, \qquad \gamma_- = -k^2. \tag{29}$$

This dispersion equation is similar to the equation for the Rossby waves for inhomogeneous rotation of the Earth or other systems. The wavenumber $k_r(t)$ is no longer fixed as in the previous case (18) but it has a time dependent value. As a consequence, the point $\Im m(\gamma)$ or $\Re e(\gamma)$ will move along the branches (similar to the branches on Figs. 3–5) with time because γ is a function of $k_r(t)$. Chagelishvili and Chkhetiani (1995) have proved that, under the influence of a shear motion, the frequencies of the Rossby waves and inertial waves will be modified to take the same values. This circumstance leads to an energy exchange between different modes in the flow. The same mechanism of the energy exchange is characteristic for system (26).

Suppose that we start the motion near the intersection point; one mode is unstable and starts to grow, while the second mode dissipates. In the intersection point their frequencies are very close to each other and a resonance interaction may take place. In this case the dissipative mode loses the main part of its energy. Thus, we have found a mechanism for the instability which may be responsible for transport and exchange of energy and angular momentum.

If we analyze the solutions of system (26) we notice that axial flow leads to a strong differentiation in the energy growth of the perturbations depending on the axial level. This dependence is represented by two Reynolds numbers in Fig. 6. This asymmetry in the energy growth in dependence on the axial level can raise the process of the symmetry breaking in the Taylor–Couette system in short cylinders.

We can assume that the same mechanism also works without any axial flow in the system. Consider two symmetrical counter-rotating Taylor vortices in the annulus. In this case a radial distribution of the axial velocity component is inhomogeneous in the annular gap and the axial velocity component goes in opposite directions in different parts of the annular gap. If a small perturbation amplifies the circulation in one of the vortices for a small interval of time, the radial gradients of the axial velocity will appear in different parts of the gap. Therefore, the degree of growth of perturbations in the continuous spectrum will be different in the two parts of the gap and the faster-growing perturbation can trigger an irreversible process of symmetry breaking.

5. A symmetry breaking and helicity conservation law

In the classical Taylor–Couette problem of pure rotation of one or both cylinders, the system possesses $\mathbf{Z}_2$ and $\mathbf{SO}(3)$ symmetries. The implementation of an axial flow immediately destroys the $\mathbf{Z}_2$ mirror symmetry. The axial perturbation flow amplifies inhomogeneously different intrinsic modes in the evaluated states, as proved in the previous section. This results in a rich variety of super critical stationary and quasiperiodic states. This symmetry breaking for short cylinders can be considered as the emergence of certain helicity states.

Helicity is a topological characteristic of flow, and it is the second inviscid integral invariant for the Euler equations. Helicity is defined by

$$\mathscr{H} = \int_V \mathbf{u}\cdot[\nabla\times\mathbf{u}]\,\mathrm{d}V, \tag{30}$$

in which the vector $\Upsilon \equiv \nabla\times\mathbf{u}$ defines the vorticity of the flow. The helicity is pseudo-scalar due to

$$\mathscr{H}(-\mathbf{r}) = -\mathscr{H}(\mathbf{r}).$$

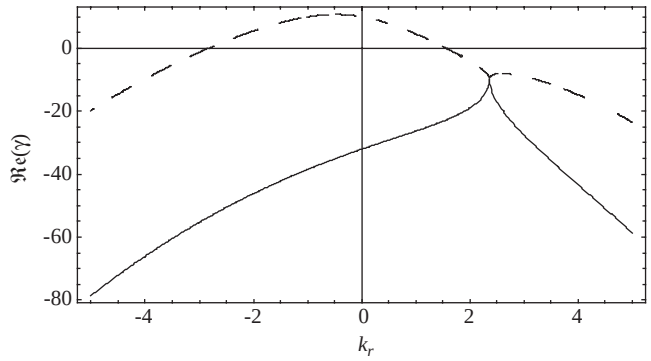

Fig. 3. The real part $\Re e(\gamma)$ of the increment γ as a function of k_r for $z = 0.25$, $r = 0.50$, $k_z = -2.00$, $\mathrm{Re} = 110$.

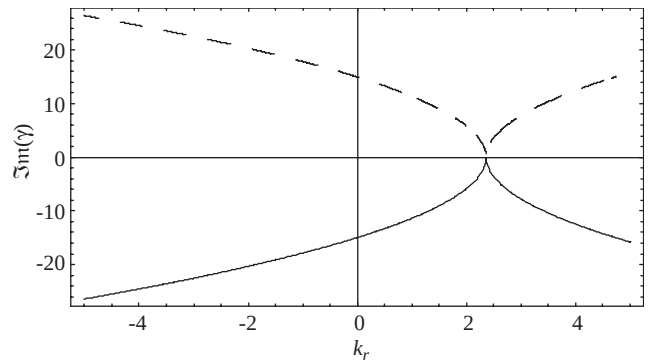

Fig. 4. The imaginary part $\Im m(\gamma)$ of the increment γ as a function of k_r for $z = 0.25$, $r = 0.50$, $k_z = -2.00$, $\mathrm{Re} = 110$.

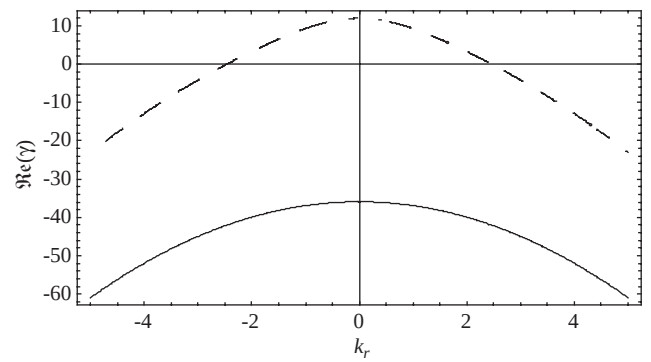

Fig. 5. The real part $\Re e(\gamma)$ of the increment γ as a function of k_r for $z = 0.50$, $r = 0.5$, $k_z = -2.0$, $\mathrm{Re} = 110$.

It is well known that helicity is an important quantity in the study of dynamics and stability of complicated vortex structures and flows. States with maximal helicity have minimal energy (Moffat and Tsinober, 1992; Chkhetiani, 2001; Chkhetiani et al., 2003).

In the same way as we procure the evolution equation for the energy of the system

$$\partial_t \mathscr{E} = \oint_S p \cdot \mathbf{u}_\mathbf{n} \, \mathrm{d}S - \nu \int_V [\nabla \times \mathbf{u}]^2 \, \mathrm{d}V,$$

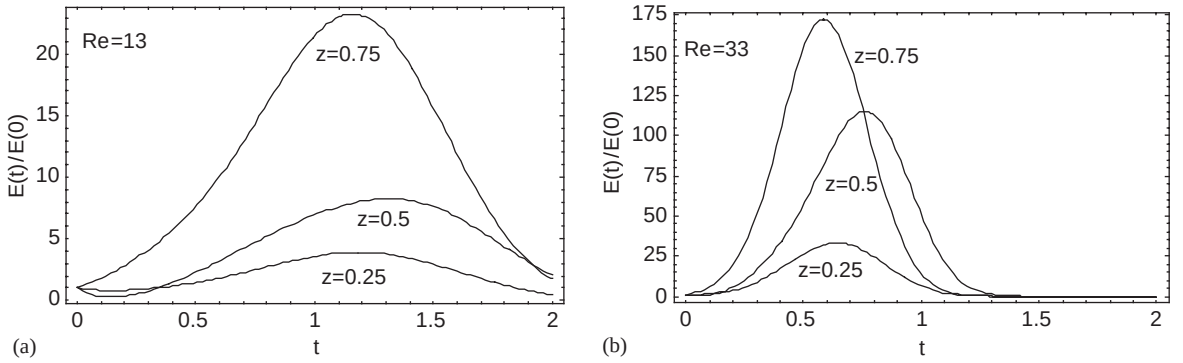

Fig. 6. The time-dependent energy growth for $\Gamma = 1$, $\zeta = 0.1$, $r = 0.5$, $k_r(0) = 1.0$, $k_z = -1$, $\widehat{\Psi}(0) = 1.0$, $\widehat{v}(0) = 1$ for different levels of z, $z = 0.25,\ 0.50, 0.75$.

we obtain the following evolution equation for the helicity:

$$\partial_t \mathscr{H} = \oint_S [\nabla \times \mathbf{u}]_\mathbf{n} \left(\frac{\mathbf{u}^2}{2} - \frac{p}{\rho} \right) \mathrm{d}S - \nu \int_V [\nabla \times \mathbf{u}] \cdot [\nabla \times [\nabla \times \mathbf{u}]] \, \mathrm{d}V, \tag{31}$$

in which $\mathbf{n}$ is the unit normal vector orthogonal to the boundary surface S.

For inviscid fluids the right-hand side of Eq. (31) is reduced to the first term. Helicity is conserved if the normal component of the vorticity on the boundary surface disappears, $[\nabla \times \mathbf{u}]_\mathbf{n} = 0$, or if there is a potential flow. Let S include a bounded volume of an ideal fluid with $\Upsilon \neq 0$ and $\mathscr{H} \neq 0$; then, during motion, helicity will be conserved. For fluids with very small viscosity $\nu \neq 0$, the helicity is no longer conserved but changes very slowly due to the negligibility of the second term in Eq. (31). As a consequence, for large Reynolds numbers we can treat the helicity as an approximately conserved quantity.

In a classical Taylor–Couette system with mirror symmetric boundary conditions we expect an even number of counter-rotating vortices. The growth of anomalous modes and the phenomenon of the appearance of time-dependent states can be considered as a mirror symmetry-breaking process and a development of states with a definite sign of the helicity. Let us represent the helicity in the cylindrical coordinate system and reduce the formula to the case of short cylinders. The components of the vorticity Υ are

$$\Upsilon_r = -\partial_z v, \quad \Upsilon_\theta = \partial_z u - \partial_r w, \quad \Upsilon_z = \partial_r v + \frac{u}{r}. \tag{32}$$

Using expressions (32) we find for the helicity $\mathscr{H}$ in the axisymmetrical case the convenient representation

$$\mathscr{H} = 4\pi \int \int_S \left(v \partial_z u + w \partial_r v + \frac{wv}{r} \right) r \, \mathrm{d}r \, \mathrm{d}z.$$

For a narrow annular gap with $\eta \sim 1$ and $R \gg 1$, we can approximate the formula for the helicity by

$$\mathscr{H} \cong 4\pi R \int \int_S \left(v \Upsilon_\theta + \frac{wv}{r} \right) \mathrm{d}r \, \mathrm{d}z \approx 4\pi R \int \int_S v \Upsilon_\theta \, \mathrm{d}r \, \mathrm{d}z.$$

The axial flow generates a constant stream of helicity and angular momentum through the annulus. It is an important source of symmetry-breaking in the system.

6. Numerical facilities

Major advances in computer technology and numerical techniques have made it possible to propose an alternative or at least a complementary approach to the classical and analytical techniques used in laboratory experiments. Computational fluid dynamics becomes part of the design process. But discontinuities or deep gradients lead to computational difficulties in the classical finite difference methods, although for the finite element methods a suitable variational principle is often not given. Therefore, we consider the finite volume methods, based on the integral form throughout the cell, instead of the differential equation. Rather than a point-based approximation on grid points, we

break the domain into *grid cells* and approximate the total integral over each grid cell. This is the *cell average*, which equals this integral divided by the volume of the cell.

We consider the axial symmetric case as well as the full 3-D flow in the annulus. The numerical method allows us to choose a so-called segregated or a coupled solver. The simulation process consists of [see, e.g., Fröhner (2002)]:

(i) division of the domain into discrete control volumes (construction of the computational grid);

(ii) integration of the governing equations (in axial-symmetric or in full 3-D form) into the individual control volumes to construct algebraic equations for the discrete variables (velocity, pressure, temperature and other parameters);

(iii) linearization and solution of the algebraic system to yield updated values of the variables.

Both the numerical methods of the segregated and the coupled solvers employ a similar finite volume process, but the approach used to linearize and solve the equations is different.

The FLUENT 5.5/6.0 (FLUENT 6.0 User's Guide, 2001) simulation and post-processing program was used for the numerical calculation of the flow. The unsteady 2-D axisymmetric or 3-D version of the Navier–Stokes equations is solved as described using finite volume discretization on a structured quadrilateral grid (see Fig. 7).

The finite volume method has a first order upwind scheme and constant relaxation factors, while the SIMPLE procedure for the pressure-velocity coupling is applied.

The grid is generated with the help of GAMBIT program and characterized by a large difference (100 times) between boundary edges. It was possible, however, to save the grid structure and the quadrilateral. The smallest inflow and outflow faces of the grid are divided uniformly by 20 nodes, whereas the nodes in the bigger geometry of the slits are concentrated near the boundary, because some vortices may arise when the Reynolds number is large (Ladyshenskaya, 1969). The major volume of the annular gap is divided 50×70 nodes, uniformly in the axial direction and linear condensing in the radial direction.

Next, we designed a 2-D axisymmetric model, using a rotating reference frame. The time step was selected to be $\frac{1}{80}$ of a single rotation. This dividing helps determine the flow motion state in the quarters of the rotation circle ($\theta = 0, \pi/2, \pi, 3\pi/2$). Each time step includes 30 iterations or fewer if the solution converges with the residual of order $\mathcal{O}(10^{-5})$.

The plane of the 3-D grid corresponding to the 2-D axisymmetric model has to be coarser, due to the large diameter of the inner cylinder and the resulting large number of cells in the projection on the (r, θ)-plane. There are only 10 nodes on the inflow and outflow faces in the conical tapering of the slits and 25×30 in the annulus of the slits (see Fig. 8).

This results in 1 087 040 hexahedral cells, which is close to the limit for computation and post-processing on a single processor in an acceptable time. Another, more complicated 3-D simulation would be possible using parallel computing (Myrnyy, 2001). Such a program is usually written with the help of Message Passing Interface (MPI-2, 1997) or some other specific approaches Mirniy and Fröhner (2001). This is the aim of further investigations and developments.

Some test simulations have shown that the 3-D case is not sensitive enough to determine very small scale instabilities correctly. The results of the 3-D and 2-D axisymmetric simulations on the same grid, however, are equivalent. This was verified using the same coarser grid for the 2-D case or by solving the stationary problem without instabilities. A finer grid for the 2-D axisymmetric case, by contrast, does not provide more substantial changes to the behavior of the unstable flow. Therefore, the 2-D axisymmetric case (see Fig. 7) with 7690 quadrilateral grid cells is chosen and can be considered for all computations with similar geometry, without loss of accuracy.

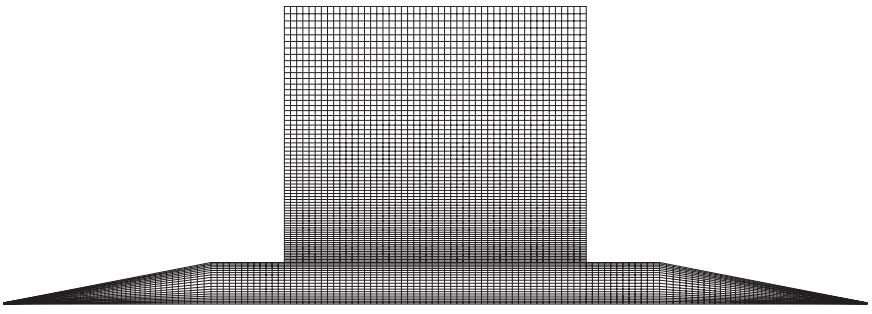

Fig. 7. 2-D structural grid for the annulus and the slits with 7690 quadrilateral cells.

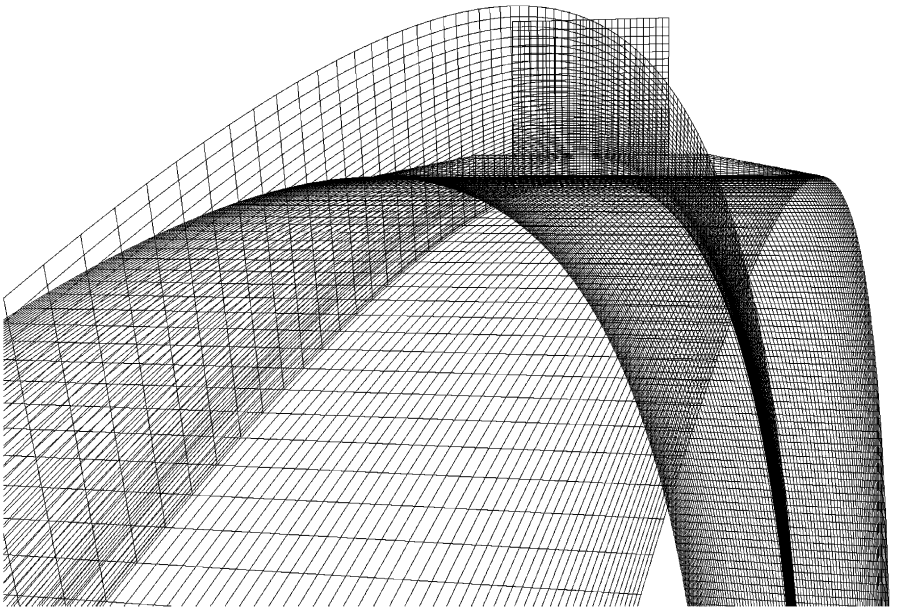

Fig. 8. 3-D grid with 1 087 040 hexahedral cells.

7. Pattern structure in the annulus under influence of the axial flow

In numerical experiments which simulated the flow in the annular gap as in Fig. 1, and in more detail in Fig. 7, both axial symmetrical and 3-D cases were studied.

The analytical part of the paper deals with a simple geometry with a rectangular cross-section in order to make the problem analytically manageable, whereas the numerical study is done for a region with narrow slits. These slits are absolutely crucial for any real experimental situation as inlet and outlet of the axial flow. Slits do exist in any real experiment, at the very least due to the sealing rings at the end of the cylinder caps.

Three-dimensional calculations had been prepared for a large number of examples. It became apparent, however, that no torsion or other remarkable 3-D effects arose in the system for $\mathrm{Re} \leqslant 6000$. Therefore, for further numerical investigations we used the axisymmetrical case, which saved both time and computer capacity. As a graphical representation of results in 3-D are insufficiently detailed when portrayed on paper, we give only one, Fig. 9, to give an impression of the process under investigation.

In all investigations the inner cylinder rotates with the same azimuthal velocity $V_0 = 2\pi\omega r_{\mathrm{in}}$ on the surface of the inner cylinder. We used this value to render other velocities dimensionless. In all figures (Fig. 9), the weak axial flow moves from left to right. The entrance and exit slits in the ends of conical tapering have the radius ratio $\tilde{\eta} = 0.99992$.

We found that four different flow states exist, with typical patterns depending upon the relation between azimuthal and axial Reynolds numbers. The azimuthal Reynolds number Re_{az} is defined by $\mathrm{Re}_{az} = V_0\, d/v$ and coincides with the previously introduced Reynolds number Re multiplied by 2π (see Section 4.1). The axial Reynolds number is defined by $\mathrm{Re}_{ax} = w_{\max}\, d/v$.

We studied a pure rotation and then switched on an axial flow to investigate the sensitivity of the flow patterns to small axial perturbations. The pattern structure is very sensitive to the presence of an axial flow. We induced a very weak axial flow with $\mathrm{Re}_{ax} \ll \mathrm{Re}_{az}$, nevertheless the pattern structure changed immediately under the influence of the axial flow. We studied the states distribution in the regions $\mathrm{Re}_{az} \in [0, 12\,000]$ and $\mathrm{Re}_{ax} \in [0, 10]$. The results for the most interesting part are that for $\mathrm{Re}_{az} \in [0, 2500]$ and $\mathrm{Re}_{ax} \in [0, 1]$; they are represented in the schematic diagram of Fig. 10.

Let us consider the case of pure rotation without any axial flow. The most probable state for a short cylinder with an aspect ratio $\Gamma \sim 1$ can be described as follows: the nearly quadratic cross-section of the annulus is filled with two counter-rotating stable Taylor vortices, as represented in Fig. 11.

We proved that this structure remains mirror-symmetric for a large region of azimuthal Reynolds numbers, $\mathrm{Re}_{az} \in [0, 2500]$. The investigated states are denoted in Fig. 10 by boxes, $\square$, on the horizontal axes. All of them

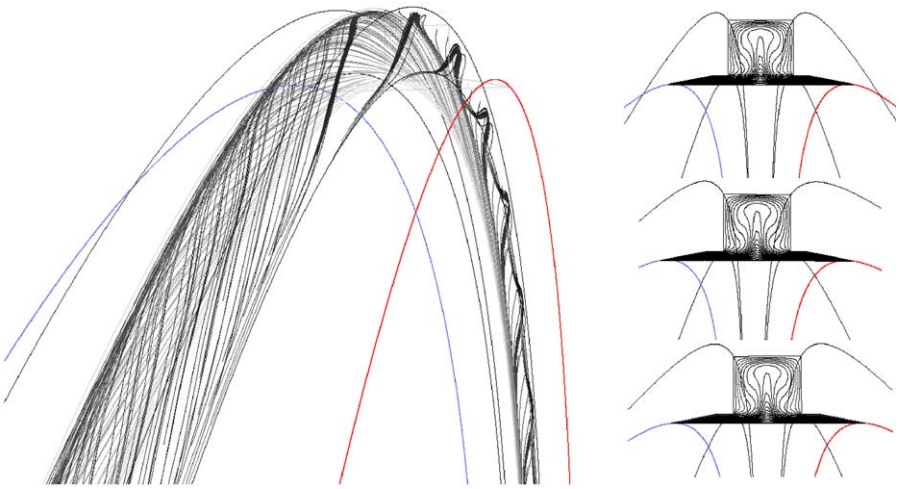

Fig. 9. Three-dimensional simulation of the two symmetrical stationary vortices. Only one of the vortices is represented to avoid an overload in the figure on the left. The counter lines of the velocity magnitude are given in the 3-D case on the left and in cross-sections shown on the right for $\theta = 0, \pi/2, \pi$, where $v = 0.1(10^{-3}\,\mathrm{m}^2/\mathrm{s})$, $w = 0.016$, $u_{\max} = 0.060$, $\mathrm{Re}_{az} = 1256.0$, $\mathrm{Re}_{ax} = 0.1$.

have quite similar structures: two stationary Taylor vortices in the annulus, raised to very high azimuthal Reynolds numbers.

An augmentation of the azimuthal Reynolds numbers leads to a second state in the annulus. For very large azimuthal Reynolds numbers $\mathrm{Re}_{az} > 4000$, the intrinsic instabilities give rise to perturbed states with many small vortices. This flow pattern can be interpreted as a region with a fine-grained structure overlaid with a large-scale structure—three Taylor-like vortices [see Fig. 12].

Consider now the onset on an axial flow with relatively small velocity. The existence of the axial flow can be understood as a small perturbation of the base flow with pure azimuthal velocity. In the region of the azimuthal Reynolds numbers $\mathrm{Re} \leqslant 1500$, the axial flow promotes the counter-rotating Taylor vortices to move in the same direction. As a result, the annulus will be filled for very small axial amplitudes of the axial flow with one stable vortex (see Fig. 13). With the introduction of axial flow, we see the abrupt change in the pattern structure as it goes from two stable Taylor vortices to one. This is the third pattern structure observed in this system; it is denoted by • in Fig. 10.

In the region of the Reynolds numbers $\mathrm{Re}_{az} \sim 1500$, $\mathrm{Re}_{ax} \sim 0,4$ there exists a branch point in which three possible flow states meet. For all axial Reynolds numbers $0.05 < \mathrm{Re}_{ax} < 4$ and $\mathrm{Re}_{az} < 1500$, it is the first branch which is characterized by one stable vortex in the annulus (see Fig. 13).

For $1250 < \mathrm{Re}_{az} < 2400$ and for the small axial Reynolds numbers $0 < \mathrm{Re}_{ax} < 0.64$, a second branch with two stable Taylor vortices appears (see Fig. 11). For $\mathrm{Re}_{az} > 1500$ and $0.3 < \mathrm{Re}_{ax} < 0.9$, the third branch appears with two quasiperiodic natural oscillating vortices (see Fig. 14).

This branch represents nonstationary states. The energy and momentum of the system also show typical quasiperiodic oscillations. The time dependence of energy is given in Fig. 15. The time dependence of the angular momentum has quite the same form. In order to make energy dimensionless, we divided it by its value at small Reynolds numbers, i.e. at $\mathrm{Re}_{az} = 251.2$, $\mathrm{Re}_{ax} = 0.02$. In Fig. 15 we also see that maximal values for the energy are smaller in the perturbation state as in the nonperturbed flow.

We shall distinguish two different types of energy in the system: the rotation or toroidal energy, defined by

$$E_{\mathrm{tor}} = 2\pi \int v^2 r \,\mathrm{d}r \,\mathrm{d}z;$$

and the energy shared by axial and local radial flow in the system

$$E_{\mathrm{pol}} = 2\pi \int (u^2 + w^2) r \,\mathrm{d}r \,\mathrm{d}z,$$

also called poloidal energy. Correspondingly with Reynolds numbers, the toroidal energy is three orders larger than the poloidal energy. But the intrinsic instabilities in the system lead to steady energy exchange between different motion types. This exchange we demonstrate by a parametric representation of the plane of both energies in Fig. 16.

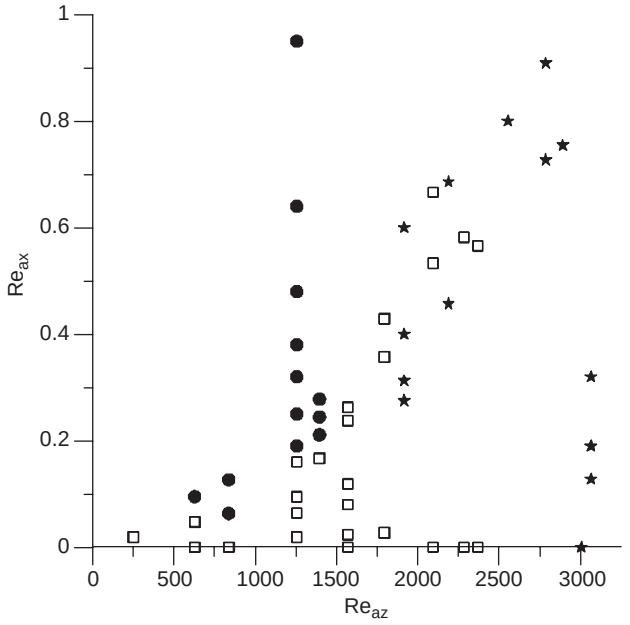

Fig. 10. The dependence of pattern distribution on the azimuthal Re_{az} and axial Re_{ax} Reynolds numbers. Two Taylor vortices in the annulus are denoted by □, one stable vortex by •, natural oscillation states of two vortices by ⋆.

The flow field between differently shaped bodies of revolution were rarely studied either experimentally or theoretically. The experimental work devoted to the case which is somewhat analogous to our case of motion in the conical slits at the caps of cylinders was done by Wimmer (2000). For a rotating cylinder in a stationary cone he proved that, due to the non-constant gap, different types of motion can coexist in the gap. By the growth of the Reynolds numbers the first vortices appear at the location of the largest gap size and are distorted as they develop a larger axial extension. The numerical studies in our geometry confirm this statement, as can be seen in Fig. 12.

8. Conclusions

We studied the Taylor–Couette flow under the imposition of a weak axial flow with a constant velocity w_0 in the case of a very short cylinder with $\Gamma = 1.02$ within a narrow annulus gap $\eta = 0.95356$.

We have assumed that the outer cylinder is at rest and the inner cylinder turns at the constant rate ω. The ingoing and outgoing gaps for the axial flow are very thin cylindrical slits which direct the axial flow in a thin layer along the surface of the inner rotating cylinder.

This is the first work in which the influence of the axial flow in a thin layer along the surface of the inner cylinder is considered. The previous work by Chandrasekhar (1961), Weisberg et al. (1997) and Ludwieg (1964) studied an axial flow that fills the full cross-sections between the cylinders.

A further important feature is that we found a rich family of flow states in a very narrow annulus gap $\eta = 0.95356$, contrary to general expectations.

A convenient asymptotic representation for the azimuthal component of the exact steady solution of the Taylor–Couette problem was found in the case of closed short cylinders $\Gamma \sim 1$, $R \gg 1$ (Section 3). The approximate solution we found, Eq. (5), will be an exact solution of the Navier–Stokes equations for infinitely large viscosity or for $\mathrm{Re} \to 0$. For finite Reynolds numbers, a flow in a thin layer can emerge along the caps of the cylinder hence the fluid motion in the cylinder will be no more unidirectional, and radial and axial components can arise. We estimated the radial and axial components of the velocity. At first it seems that in cases of strong non-linear motion, the estimation $u/V_0 \sim R^{-1/2}$, $w/V_0 \sim R^{-1/2}$ must hold. This follows from the comparison of the non-linear terms in the Navier–Stokes equations. But the numerical computations for the short cylinders with $R \gg 1$ and large Reynolds numbers lead to another estimation, $u/V_0 \sim R^{-1}$, $w/V_0 \sim R^{-1}$, which can be obtained from the Navier–Stokes equations in cases of very

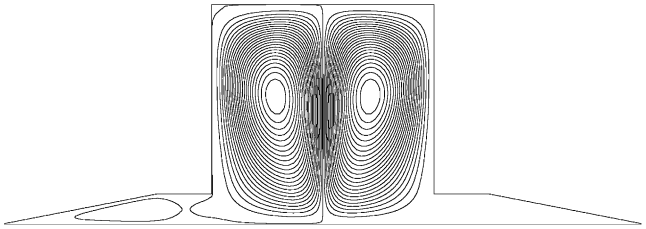

Fig. 11. Two symmetrical stationary Taylor vortices which are denoted by □ in Fig. 10. Here, $v = 0.8(10^{-4}\ \mathrm{m}^2/\mathrm{s})$, $w = 0$, $u_{\max} = 0.07$, $\mathrm{Re}_{az} = 1570$, $\mathrm{Re}_{ax} = 0$.

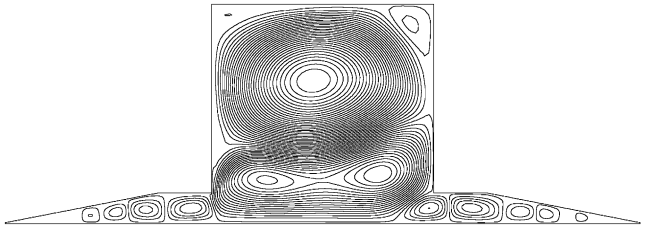

Fig. 12. A fine-grained structure of small vortices overlaid by large scale vortices. Here, $v = 0.1(10^{-4}\,\mathrm{m}^2/\mathrm{s})$, $w = 0$, $u_{\max} = 0.04$, $\mathrm{Re}_{az} = 12560$, $\mathrm{Re}_{ax} = 0$.

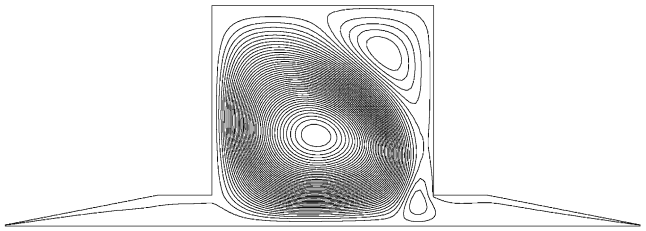

Fig. 13. One large stationary vortex nearly fills the entirety of the annulus (these states are denoted in Fig. 10 by •). Here, $v = 0,1(10^{-3}\ \mathrm{m}^2/\mathrm{s})$; $w = 0,05$; $u_{\max} = 0,04$; $\mathrm{Re}_{az} = 1256$; $\mathrm{Re}_{ax} = 0,32$.

large viscosity. In Fig. 17 we represent the radial component of the dimensionless velocity only. For the other velocity component, the distribution pattern is quite the same.

From the estimations obtained, it follows that the azimuthal component of the velocity has the main influence on the stability of the system. Consequently, we can use for our qualitative stability analysis the approximate solution we found.

We made a numerical simulation of the flow in presence of slits, i.e. without singularities in the corners of the domain, and the azimuthal component of the velocity turned out to be very close to the approximate azimuthal solution. The other two components of the velocity are small and thus not important.

The stability analysis done in Section 4 showed that the inhomogeneity of the base flow in the radial direction as well as the axial flow cause a perturbation of the same type as in Rossby waves. We proved that the $\mathbf{Z}_2$-symmetry breaking due to the axial flow in the Taylor–Couette flow is, at the same time, breaking the helicity symmetry (Section 5). States with non-zero helicity can accrue in the system (Section 7). The energy oscillations in the case of unsteady patterns with natural oscillations as in Fig. 15 correspond to helicity oscillations in the system. This can be seen from Fig. 14.

We are confident that up to the limits of numerical accuracy, the states are axially symmetric. The axial symmetry will be conserved in cases of very short cylinders with weak axial flow. This situation was also proven in experiments [see Mullin et al. (2002), Furukawa et al. (2002), Furukawa (2002), Watanabe et al. (2002) and Watanabe et al. (2003)]. As we have shown in our work, the influence of the axial flow resulted in the destruction of mirror symmetry.

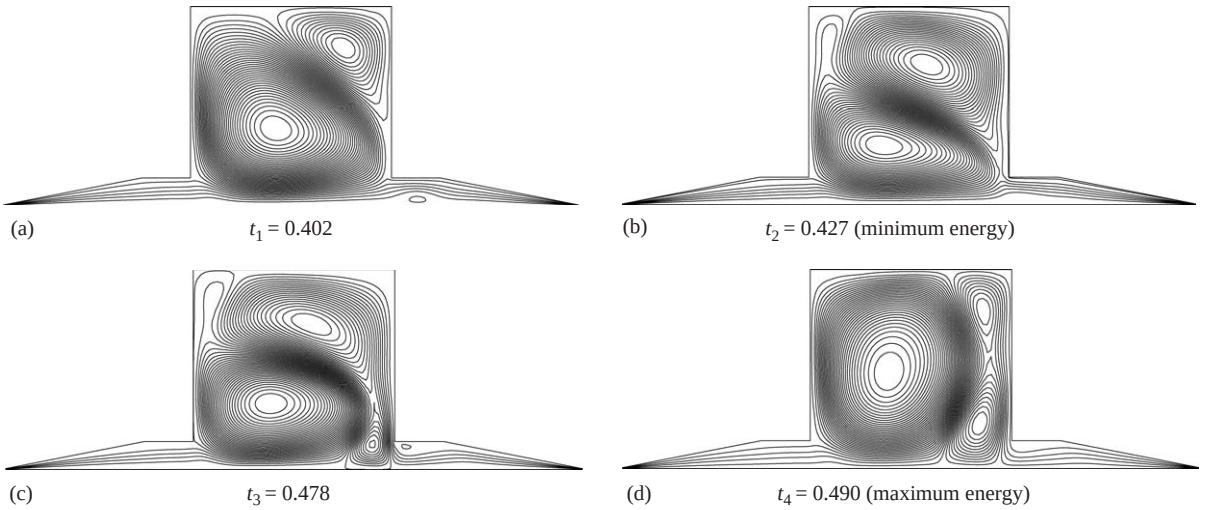

Fig. 14. The natural quasiperiodic oscillations of the two vortices in the annulus (denoted in Fig. 10 by ⋆) in four different moments of dimensionless time. Here, $v = 0.3(10^{-4}\,\mathrm{m}^2/\mathrm{s})$, $w = 0.30$, $u_{\max} = 0.05$, $\mathrm{Re}_{az} = 5108$, $\mathrm{Re}_{ax} = 6.333$.

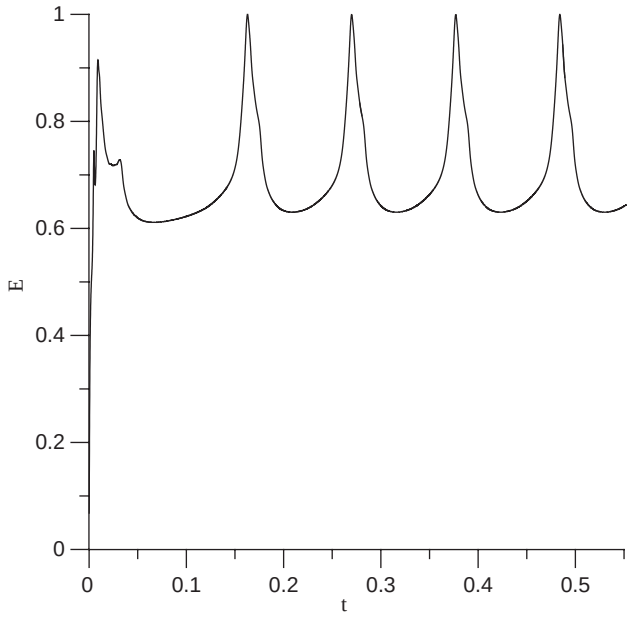

Fig. 15. The time dependence of the total energy $E(t)$ for the flow for $\mathrm{Re}_{az} = 5108$, $\mathrm{Re}_{ax} = 6,333$.

The weak axial flow in an annulus between the rotating inner cylinder and the fixed outer cylinder has several important engineering applications, particularly if the axial flow is bounded in a thin layer along the surface of the rotating cylinder. We studied this case and proved that the axial flow stabilizes the motion and that in a system with very narrow annulus different supercritical states are possible (Section 7). We remark that experiments in short cylinders with an aspect ratio of $\Gamma \sim 1$ without any axial flow showed a poor variety of states (Furukawa, 2002; Watanabe et al., 2002). But for smaller aspect ratios, all the states which we described in our case can be observed. This behavior of the Taylor–Couette system can be interpreted as follows. The influence of the weak axial flow along the

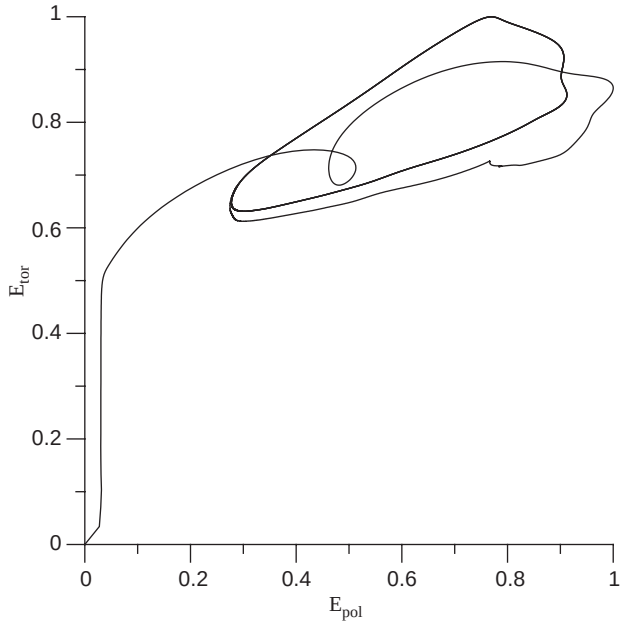

Fig. 16. The parametric representation of the energy exchange between E_{tor} and E_{pol} in the plane of the two energies for $\mathrm{Re}_{az} = 5108$, $\mathrm{Re}_{ax} = 6, 333$.

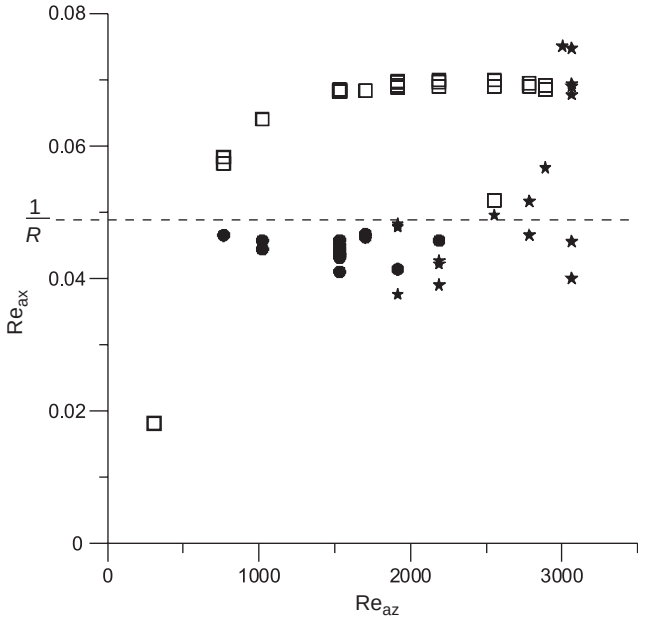

Fig. 17. The distribution of the radial component of the dimensionless velocity max $\tilde{u}$ in the Taylor–Couette flow for different states dependent upon the Reynolds numbers Re_{az} and Re_{ax}. Two Taylor vortices in the annulus are denoted by □, one stable vortex by •, natural oscillation state of two vortices by ⋆.

surface of the inner cylinder can be considered as a change in the geometry, i.e., as a shortening of the axial length of the cylinder. This interpretation is supported by simple estimations.

We observe that the self-oscillating flow regime turns abruptly and strongly (see Fig. 15) in our case, contrary to the experiments of Furukawa (2002), Watanabe et al. (2002, 2003) and where the changes were monotonic.

For technical applications it is important to describe not only the velocity field but also the pressure distribution in the device. The pressure differences in the annulus coming from the vortex motion can be estimated as R^{-1} of the pressure difference corresponding to the axial flow.

Acknowledgments

The authors are grateful M.V. Babich, E.-P. von Bergen, Ch. Egbers, S.K. Matveev, V.M. Ponomarev, A.I. Shafarevich and G. Windisch for interesting and fruitful discussions. The work was kindly supported by the BMBF–project Grant Number PIM3CB under the leadership of S. Pickenhain.

References

Aitta, A., Ahlers, G., Cannell, D.S., 1985. Tricritical phenomena in rotating Couette–Taylor flow. Physical Review Letters 54, 673–676.

Benjamin, T.B., Mullin, T., 1981. Anomalous modes in the Taylor experiment. Proceedings of the Royal Society of London, Series A—Mathematical Physical and Engineering Sciences 377, 221–249.

Benjamin, T.B., Mullin, T., 1982. Notes on the multiplicity of flows in the Taylor experiment. Journal of Fluid Mechanics 121, 219–230.

Bhattacharjee, J.K., 1987. Convection and Chaos in Fluids. World Scientific Publishing Co., Singapore.

Bordag, L.A., 2001. Neue Ansätze zur Modellierung drei-dimensionaler viskoser Strömungen am Beispiel der Stevenrohrabdichtung. In Proceedings of 4. Tagung der Deutschen Sektion der EWM in Chemnitz, Chemnitz, pp. 3–7.

Buttler, K.M., Farrel, B.F., 1992. Three-dimensional perturbations in visouse shear flow. Physics of Fluids A 4, 1627–1650.

Chagelishvili, G.D., Chkhetiani, O.G., 1995. Linear transformation of Rossby waves in shear flows. JETP Letters 62, 314–321.

Chagelishvili, G.D., Rogava, A.D., Tsiklauri, D.G., 1996. Effect of coupling and linear transformation of waves in shear flows. Physical Review E 53, 6028–6031.

Chandrasechar, S., 1960. The hydrodynamic stability of viscous flow between coaxical cylinders. Proceedings of the National Academy of Sciences of the USA 46, 141–143.

Chandrasekhar, S., 1961. Hydrodynamic and Hydromagnetic Stability. Clarendon Press, Oxford.

Chkhetiani, O.G., 2001. On the helical structure of the Ekman boundary layer. Izvestiya Atmospheric and Oceanic Physics 37, 569–575.

Chkhetiani, O.G., Ponomarev, V.M., Khapaev, A.A., 2003. Role of helicity in the formation of secondary structures in the Ekman boundary layer. Izvestiya Atmospheric and Oceanic Physics 39, 391–400.

Cliffe, K.A., Mullin, T., 1985. A numerical and experimental-study of anomalous modes in the Taylor experiment. Journal of Fluid Mechanics 153, 243–258.

Cliffe, K.A., Kobine, J.J., Mullin, T., 1992. The role of anomalous modes in Taylor–Couette flow. Proceedings of the Royal Society of London, Series A—Mathematical Physical and Engineering Sciences 439, 341–357.

Di Prima, R.C., 1960. The stability of viscous flow between rotating coaxical cylinders. Journal of Fluid Mechanics 9, 621–631.

FLUENT 6 User's Guide, 2001. Fluent Inc., 10 Cavendish Court, Lebanon, NH, USA.

Fröhner, M., 2002. Numerical simulation on parallel computer cluster in fluid dynamics. The Bulletin of KazNU, Mathematics, Mechanics and Informatics Issue 4 (32), 84–92.

Furukawa, H., 2002. Mode formation and bifurcation in Taylor vortex flow with small aspect ration. Nagoya University, Japan. hiroyuki@info.human.nagoya-u.ac.jp

Furukawa, H., Watanabe, T., Toya, Y., Nakamura, I., 2002. Flow pattern exchange in the Taylor–Couette system with a very small aspect ratio. Physical Review E 65, 036306-1.

Goldreich, P., Schubert, G., 1967. Differential rotation in stars. Astrophysical Journal 150, 571.

Gustavsson, L.H., 1979. Initial value problem for boundary layer flows. Physics of Fluids 22, 1602–1605.

Hristova, H., Roch, S., Schmid, P.J., Tuckerman, L.S., 2002. Transient growth in Taylor–Couette flow. Physics of Fluids 14, 3475–3484.

Hu, H.C., Kelly, R.E., 1995. Effect of a time-periodic axial shear flow upon the onset of Taylor vortices. Physical Review E 51, 3242–3251.

Ji, H., Goodman, J., Kageyama, A., 2001. Magnetorotational Instability in a Rotating Liquid Metal Annulus. Monthly Notices of the Royal Astronomical Society Aims & Scope 325, L1–L5.

Joseph, D.D., 1976. Stability of fluid motions, I, II. In: Colleman, B.D. (Ed.), Springer Tracts in Natural Philosophy, vols. 27, 28. Springer, Berlin, Heidelberg, New York.

Kageyama, A., Ji, H., Goodman, J., 2004. Numerical and experimental investigation of circulation in short cylinders. Journal of Physical Society Japan 73, 2424–2437.

Ladyshenskaya, O.A., 1969. The Mathematical Theory of Viscous Incompressible Flow, second ed. Gordon and Breach Science Publishers, New York.

Lebovitz, N., Lifschitz, A., 1993. Local hydrodynamic instability of rotating stars. Astrophysical Journal 40, 603–614.

Lifschitz, A., 1991. Essential spectrum and local stability condition in hydrodynamics. Physics Letters A 152, 3–4, 199–204.

Lifschitz, A., Hameiri, E., 1993. Localized instabilities of vortex rings with swirl. Communications on Pure and Applied Mathematics 46, 1379–1408.

Lominadze, D.G., Chagelishvili, G.D., Chanishvili, R.G., 1988. The evolution of nonaxisymmetric shear perturbations in accretion disks. Soviet Astronomy Letters 14 (5), 364–367.

Ludwieg, H., 1964. Experimentelle Nachprüfung der Stabilitätstheorien für reibungsfreie Strömungen mit schraubenlinienförmigen Stromlinien. Zeitschrift für Flugwissenschaften und Weltraumforschung 12, 304–309.

Lueptow, R.M., 2000. Stability and experimental velocity field in Taylor–Couette flow with an axial and radial flow. In: Egbers, Ch., Pfister, G. (Eds.), Physics of Rotating Fluids. Springer, Berlin, pp. 137–155.

Marques, F., Lopez, J.M., 1997. Taylor–Couette flow with axial oscillations of the inner cylinder: floquet analysis of the basic flow. Journal of Fluid Mechanics 348, 153–175.

Meseguer, Á., 2002. Energy transient growth in the Taylor–Couette problem. Physics of Fluids 14, 1655–1660.

Meseguer, Á., Marques, F., 2000. Axial effects in the Taylor–Couette problem: spiral-Couette and spiral-Poiseuille flows. In: Egbers, Ch., Pfister, G. (Eds.), Physics of Rotating Fluids. Springer, Berlin, pp. 118–136.

Milne-Thomson, L.M., 1996. Theoretical Hydrodynamics, Dover Publications, New York, p. 477.

Mirniy, V., Fröhner, M., 2001. On a computer program for modeling the molecular gas dynamics with parallelization. Computer Technology 6 (3), 32–50.

Moffat, H.K., Tsinober, A., 1992. Helicity in laminar and turbulent flow. Annual Review of Fluid Mechanics 24, 281–312.

MPI-2: Extensions to the Message-Passing Interface, Message Passing Interface Forum, Version 2.0, July 18, 1997. http://www.mpi-forum.org/docs/docs.html

Mullin, T., Benjamin, T.B., 1980. Transition to oscillatory motion in the Taylor experiment. Nature 288, 567–569.

Mullin, T., Toya, Y., Tavener, S.J., 2002. Symmetry breaking and multiplicity of states in small aspect ratio Taylor–Couette flow. Physics of Fluids 14 (8), 2778–2787.

Myrnyy, V., 2001. Parallelisierung numerischer Probleme—Möglichkeiten und Grenzen, Brandenburg University of Technology, Report M-11/2001, Cottbus.

Neitzel, G.P., Kirkconnell, C.S., Little, L.J., 1995. Transient, nonaxisymmetric modes in the instability of unsteady circular Couette-flow—laboratory and numerical experiments. Physics of Fluids 7 (2), 324–334.

Reddy, S.C., Hennigson, D.S., 1993. Energy growth in viscous channel flows. Journal of Fluid Mechanics 252, 209–238.

Schaeffer, D.G., 1980. Qualitative-analysis of a model for boundary effects in the Taylor problem. Mathematical Proceedings of the Cambridge Philosophical Society 87, 307–337.

Streett, C.L., Hussaini, M.Y., 1991. A numerical-simulation of the appearance of chaos in finite-length Taylor–Couette flow. Applied Numerical Mathematics 7, 41–71.

Taylor, G.I., 1923. Stability of a viscous liquid contained between two rotating cylinders. Philosophical Transactions Mathematical, Physical and Engineering Sciences. The Royal Society, London, Series A 223, 289–343.

Vladimirov, V.A., Yudovich, V.I., Zhukov, M.Yu., Denissenko, P.V., 2001. On vortex flows in a gap between two parallel plates. Matematicheskie Metody i Vychislitelnye Experimenty 13 (2), 27–37.

Watanabe, T., Furukawa, H., Nakamura, I., 2002. Nonlinear development of flow patterns in an annulus with decelerating inner cylinder. Physics of Fluids 14 (1), 333–341.

Watanabe, T., Umemura, N., Furukawa, H., Nakamura, I., 2003. Three-dimensional numerical study on mode transitions of developing Taylor–Couette flow in very short annulus. Transaction of the Japan Society for Computational Engineering and Science, Paper No. 20030022.

Weisberg, A.Y., Kevrekidis, I.G., Smits, A.J., 1997. Delaying transition in Taylor–Couette flow with axial motion of the inner cylinder. Journal of Fluid Mechanics 348, 141–151.

Wendl, M.C., 1999. General solution for the Couette flow profile. Physical Review E 60 (5), 6192–6194.

Wimmer, M., 2000. Taylor vortices at different geometries.-212. In: Egbers, Ch., Pfister, G. (Eds.), Physics of Rotating Fluids. Springer, Berlin, pp. 194–212.